



## Original Research Paper

# Synthesis and characterization of perovskite type of $\text{La}_{1-x}\text{Ba}_x\text{MnO}_3$ nanoparticles with investigation of biological activity

Serpil Gonca <sup>a</sup>, Sadin Özdemir <sup>b,\*</sup>, Atakan Tekgül <sup>c</sup>, Cumhuri Gokhan Unlu <sup>d,\*\*</sup>, Kasim Ocakoglu <sup>e</sup>, Nadir Dizge <sup>f</sup>

<sup>a</sup> Department of Pharmaceutical Microbiology, Faculty of Pharmacy, Mersin University, Turkey, 33343 Mersin, Turkey

<sup>b</sup> Food Processing Programme, Technical Science Vocational School, Mersin University, 33343 Mersin, Turkey

<sup>c</sup> Department of Physics, Science Faculty, Bursa Uludag University, 16100 Bursa, Turkey

<sup>d</sup> Department of Biomedical Engineering, Pamukkale University, 20160 Denizli, Turkey

<sup>e</sup> Faculty of Engineering, Department of Engineering Fundamental Sciences, Tarsus University, 33400 Tarsus, Turkey

<sup>f</sup> Department of Environmental Engineering, Mersin University, 33343 Mersin, Turkey

## ARTICLE INFO

## Article history:

Received 30 May 2021

Received in revised form 23 October 2021

Accepted 29 October 2021

Available online 23 December 2021

## Keywords:

Lanthanum nanoparticles

Perovskite

Antioxidant

DNA cleavage

Antimicrobial

## ABSTRACT

The enhanced biological activity of perovskite type  $\text{La}_{1-x}\text{Ba}_x\text{MnO}_3$  ( $x = 0.2, 0.3, 0.4$ ) nanoparticle was studied based on antioxidant, antimicrobial, anti-biofilm, bacterial viability inhibition, and DNA cleavage studies. The nanoparticles were prepared by Sol-gel technique and they were analyzed on structure and morphological by XRD and SEM.  $\text{La}_{0.6}\text{Ba}_{0.4}\text{MnO}_3$  showed the highest DPPH free radical scavenging activity and iron chelating activity as 67.23% and 46.54%, respectively. All tested lanthanum nanoparticles showed good chemical nuclease activity. *C. tropicalis* was the most affected species by lanthanum nanoparticles and MIC values were 4  $\mu\text{g}/\text{mL}$ , 8  $\mu\text{g}/\text{mL}$ , and 16  $\mu\text{g}/\text{mL}$  for  $\text{La}_{0.7}\text{Ba}_{0.4}\text{MnO}_3$ ,  $\text{La}_{0.6}\text{Ba}_{0.4}\text{MnO}_3$ , and  $\text{La}_{0.8}\text{Ba}_{0.2}\text{MnO}_3$ , respectively.  $\text{La}_{0.7}\text{Ba}_{0.4}\text{MnO}_3$  exhibited the highest percentage of biofilm inhibition against *P. aeruginosa* and *S. aureus* as 99.78% and 98.38%, respectively. Cell viability assay demonstrated that  $\text{La}_{0.7}\text{Ba}_{0.4}\text{MnO}_3$ ,  $\text{La}_{0.6}\text{Ba}_{0.4}\text{MnO}_3$ , and  $\text{La}_{0.8}\text{Ba}_{0.2}\text{MnO}_3$  showed %100 cell viability inhibition after 30 and 60 min treatment.

© 2021 The Society of Powder Technology Japan. Published by Elsevier B.V. and The Society of Powder Technology Japan. All rights reserved.

## 1. Introduction

The enhanced structural, electronic and magnetic properties of perovskites composites have been of great interest in a diverse technological field, due to their unique properties. They display the regular arrangement with the general formula  $\text{ABO}_3$ , where A denotes rare earth or alkaline earth elements ion ( $A = \text{La}, \text{Pr}, \text{etc.}$ ) and B is the transition element ions ( $B = \text{Mn}, \text{Cr}, \text{etc.}$ ). In the cubic structure, the A atoms of the perovskite are located at the cube corners, B atoms at the body centers, and the oxygens at the face centers. The perovskite structure can tolerate vacancies (or partial substitution) at the A sites giving rise to non-stoichiometric compositions such as  $\text{A}_{(1-x)}\text{BO}_3$ . These vacancies add new features to the lanthanum nanoparticles.  $\text{LaMnO}_3$  perovskite structure has been mostly studied because of the behavior of the  $\text{Mn}^{3+}$  ions. Lanthanum is an abundant element than other rare earth elements as well. Partial substitution of La with divalent

ions such as Sr, Ca, and Ba in the A site of perovskite can provide to control the magnetic properties of the compound [1]. At the same time, both strong ferromagnetism and metallic conductivity can be tuned by the substitution [2,3,4]. These substitutions create a mixed valence state of  $\text{Mn}^{3+}/\text{Mn}^{4+}$ , resulting in mobile charge carriers and canting of the Mn spins. The crystal structure of the perovskite generally shows lattice distortions because of the modifications from the ideal cubic toward rhombohedral or orthorhombic due to the effect of Jahn-Teller, resulting the deformation of the  $\text{MnO}_6$  octahedra. In these perovskites, the cations vacancies directly affect the physical properties [5,6] and many authors show that the vacancies can improve their physical properties of the perovskites [7,8,9,10].

Lanthanum nanoparticles are generally synthesized using various methods such as sol-gel, hydrothermal, ball milling, solid state, etc. The sol-gel methods are the most commonly used technique because of simple and low cost synthesis route and also no need higher temperature for calcinations [11]. The perovskites are concurrently magnetic materials and they can be used as catalysts, magnetocaloric material for the cooling/heating process, magnetic hyperthermia mediate or agent [12]. The various metal or metal oxide nanoparticles such as Ag,  $\text{Al}_2\text{O}_3$  have been screened

\* Corresponding author.

\*\* Corresponding author.

E-mail addresses: [sadinozdemir@mersin.edu.tr](mailto:sadinozdemir@mersin.edu.tr) (S. Özdemir), [cunlu@pau.edu.tr](mailto:cunlu@pau.edu.tr) (C. Gokhan Unlu).

as antibacterial agents [13]. Among of these, magnetic nanoparticles are widely used in biomedical sciences due to their biocompatibility, chemical stability and magnetic behaviour [14]. Lanthanum based perovskite oxides have been the most frequently studied and have demonstrated remarkable performance in different types of catalysis such as  $\text{LaCo}_x\text{Fe}_{1-x}\text{O}_3$  [9]. Lanthanum doped  $\text{NaTaO}_3$  has been studied for photocatalytic applications [10]. Perovskites nanoparticle have a small size and high surface area to volume ratio resulting into surfaces with high free energy. To reduce these energy, high surface area becomes inclined to interact with the environment. The certain interactions have energy to overcome bandgap barrier of the nanoparticles and this causes the generation of electron-hole pair. The free electron results in production of free reactive oxygen species in the environment [15].

Since lanthanum is a biologically inert element, lanthanum compounds have been used to treat illness. For example, lanthanum carbonate has been used for an agent to binding phosphates in the cure of hyper-phosphatemia in dialyzed patients. So, the fine biological safety shows the potential of lanthanum as candidates for drug innovation. In addition, the recent research developments display that lanthanum is also involved in biochemical pathways and display well biological activity. The good biological properties of lanthanum compounds are connected to the original coordination properties of lanthanum element [16].

In this study, perovskite type  $\text{La}_{1-x}\text{Ba}_x\text{MnO}_3$  ( $x = 0.2, 0.3, 0.4$ ) nanoparticles were prepared by Sol-gel technique and they were analyzed on structure and morphological by XRD and SEM. Moreover, the enhanced biological activity of the nanoparticles was studied based on antioxidant, antimicrobial, anti-biofilm, bacterial viability inhibition, and DNA cleavage studies.

## 2. Materials and methods

### 2.1. Synthesis of perovskite type $\text{La}_{1-x}\text{Ba}_x\text{MnO}_3$ nanoparticles

$\text{La}_{1-x}\text{Ba}_x\text{MnO}_3$  ( $x = 0.2, 0.3, 0.4$ ) were prepared using sol-gel technique. Appropriate amounts of  $\text{La}(\text{NO}_2)_3$ ,  $\text{Ba}_2(\text{NO}_2)_3 \cdot 4\text{H}_2\text{O}$ , and  $\text{Mn}(\text{NO}_2)_3 \cdot 4\text{H}_2\text{O}$  were dissolved in distilled water to obtain controlled stoichiometry of the compounds. Subsequently, citric acid and ethylene glycol as to be 10% of the solution concentration were added to the mixture. A viscous residue was formed by slowly boiling the solution at 200 °C. The obtained residue was dried at 250 °C until a dry-gel. Finally, the residual precursor was burned in the air at 600 °C for 12 h to remove the organic materials produced in the chemical reactions. Then, the remain powders were ground to obtain homogeny fine powder.

### 2.2. Characterization of perovskite type $\text{La}_{1-x}\text{Ba}_x\text{MnO}_3$ nanoparticles

Structural analysis was performed using Rigaku D-max B horizontal diffractometer with  $\text{Cu K}\alpha$  radiation at room temperature. The X-ray diffraction (XRD) patterns were refined by the FullProf Software using Rietveld Refinement method. The morphologic analysis of the compounds was determined using FEI-Quanta 650 field emission scanning electron microscopy (SEM). For SEM analysis, some of the nanoparticle powders were placed on stubs attached with carbon tape and placed in the system. The measurements were taken in a vacuum environment and at electron energies 15 keV, which is the typical range for SEM. Energy dispersive X-ray analysis (SEM-EDX) analysis was carried out to investigate the surface compositions of the prepared compounds. The surface area, total pore volume, microporous volume, and pore diameters of the compounds were measured by Brunauer Emmett-Teller (BET) analysis (MicroActive for TriStar II Plus 2.00).

### 2.3. DPPH activity

The antioxidant activity of the synthesized lanthanum nanoparticles was studied by DPPH method [17]. DPPH solution was prepared by using methanol. 500  $\mu\text{L}$  lanthanum nanoparticles solution prepared at 5 different concentrations (25, 50, 100, 250, and 500 mg/L) was added to 2 mL DPPH solution. The resultant mixture was incubated at dark for 30 min at room temperature. Later, the change in color was observed of mixtures and absorbance was measured at 517 nm using UV-VIS spectrophotometer. All experiments were tested at least triple. Trolox and ascorbic acid were taken as standard. The ability to scavenge the DPPH radical was calculated using Eq. (1):

$$\text{Capacity (\%)} = \left( \frac{\text{Abs}(\text{control}) - \text{Abs}(\text{sample})}{\text{Abs}(\text{control})} \right) \times 100 \quad (1)$$

$\text{Abs}_{\text{control}}$  is control absorbance and  $\text{Abs}_{\text{sample}}$  is the absorbance value of the test compounds and DPPH after 30 min.

### 2.4. Ferrous ion chelating activity

The ferrous ion chelating activity of the synthesized lanthanum nanoparticles and EDTA were studied according to the literature [18]. EDTA solution used as a positive control. 0.5 mL of lanthanum nanoparticles prepared in different concentrations from 25 to 500 mg/L was taken and mixed with 0.05 mL of 2 mM  $\text{FeCl}_2$  solution. It was then vortexed by adding 100  $\mu\text{L}$  of 5 mM ferrous solution to the mixture and incubated at room temperature for 10 min. All experiments were tested at least triple. The absorbance values of the mixtures were measured at 562 nm and the percent of chelating activity was calculated by Eq. (2):

$$\text{Metal Chelating Effect (\%)} = \left( \frac{\text{Abs}(\text{control}) - \text{Abs}(\text{sample})}{\text{Abs}(\text{control})} \right) \times 100 \quad (2)$$

where  $\text{Abs}_{\text{control}}$  is the absorbance of the control reaction, and  $\text{Abs}_{\text{sample}}$  represents the absorbance obtained in the presence of compounds or EDTA.

### 2.5. DNA cleavage ability

Gel electrophoresis method was used to examine the effect of synthesized lanthanum nanoparticles on DNA. pBR 322 plasmid DNA (Form I) was used as DNA. Different concentrations of lanthanum nanoparticles and 0.1  $\mu\text{g}/\mu\text{L}$  DNA were mixed in PCR tubes and incubated at 37 °C for 60 min. After the incubation period, loading dye was added into the PCR tubes and the mixture was loaded on 1% agarose gel. The gel was electrophoresed for 90 min at 50 V in TAE buffer (50mMTris base, 50mMAcetic acid, 2 mM EDTA, pH:7.8).

After electrophoresis, the gels were illuminated with UV light and then photographed.

### 2.6. Antimicrobial activity

The MIC concentration of newly synthesized lanthanum nanoparticles was studied with liquid microdilution method. It has been studied with 8 strains, 3 Gram + ve, 3 Gram -ve and 2 yeast fungi. The strains used in the study were *Staphylococcus aureus* (ATCC 25923), *Enterococcus faecalis* (ATCC 29212), *Enterococcus hirae* (ATCC 10541), *Pseudomonas aeruginosa* (ATCC 27853), *Escherichia coli* (ATCC 25922), *Legionella pneumophila* subsp. *pneumophila* (ATCC 33152), *Candida tropicalis* (ATCC 750), and *Candida parapsilosis* (ATCC 22019). The test microorganisms were grown overnight for 16 h incubation at  $37 \pm 2$  °C before micro dilution study in

Nutrient Broth (NB) which contains 15 g/L peptone, 3 g/L yeast extract, 6 g/L sodium chloride, and 1 g/L glucose. The stock solution of lanthanum nanoparticles was prepared as 2048 mg/L and two-fold serial dilutions of lanthanum nanoparticles were made for the study, and then the above-mentioned microorganisms ( $3.2 \times 10^8$  CFU/mL) were added to the microplate-wells as 1% volume. Next plates left for 24 h incubation at  $37 \pm 2$  °C. All experiments were tested at least triple. At the end of the incubation period, MIC values were defined as the lowest concentration that prevented the growth of microorganisms.

## 2.7. Bacterial viability inhibition test

*E. coli* (ATCC 10536) was used in the cell viability study as a bacterial strain. After the microorganism was inoculated into NB (Nutrient Broth), it was incubated for 24 h at 37 °C at 120 rpm in a shaker-capable oven. After incubation, *E. coli* cell was collected at 5000 rpm for 5 min by centrifuge. The pellet was then washed with sterile NaCl solution (0.85% (w/v)) to clean the bacterial cell and remove residual medium. The cleaned bacterial cell pellet was suspended in 10 mL of NaCl solution. This solution was per-

formed for cell viability study. Bacterial cell pellet was treated with lanthanum nanoparticles. Same procedure was also applied with control group which was not contained lanthanum nanoparticles. They were incubated for 30 and 60 min. After that they were diluted and inoculated in a petri dish and left to incubate at 37 °C for 24 h. All experiments were tested at least triple. Then the colonies were counted and the cell viability inhibition calculated using with eq. (3).

**Table 1**

The lattice parameters of the  $\text{La}_{1-x}\text{Ba}_x\text{MnO}_3$  ( $x = 0.2, 0.3, 0.4$ ).

$\text{La}_{1-x}\text{Ba}_x\text{MnO}_3$	$x = 0.2$	$x = 0.3$	$x = 0.4$	
Phase	<i>R-3cH</i>	<i>R-3cH</i>	<i>R-3cH</i>	<i>Cmca</i>
a (Å)	5.544	5.538	5.571	5.781
b (Å)	=a	=a	=a	13.183
c (Å)	13.480	13.490	13.433	19.440
V (Å) <sup>3</sup>	358.774	358.335	360.999	1481.439
$\chi^2$	1.83	1.87	1.95	
Phase Percentage	100	100	93.65	6.35

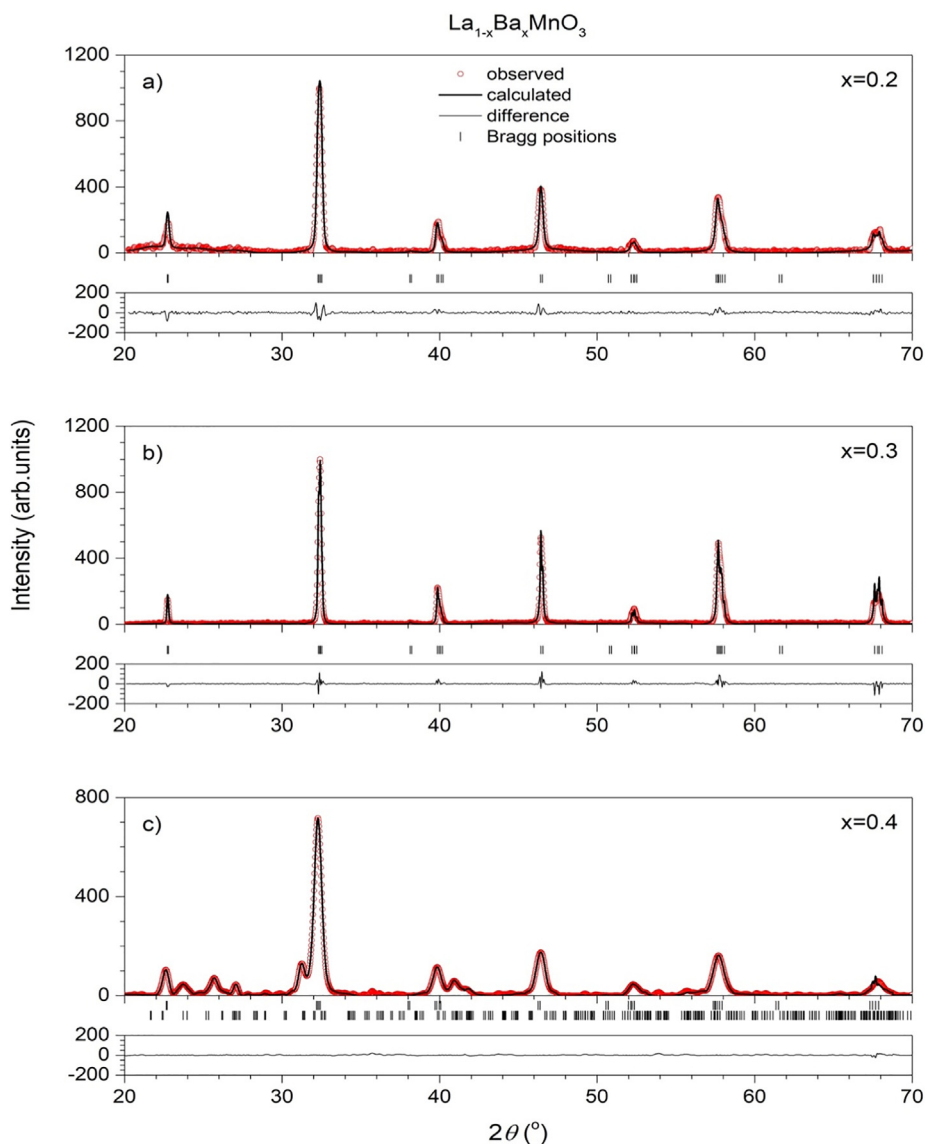


**Fig. 1.** Refined X-ray diffraction patterns for  $\text{La}_{1-x}\text{Ba}_x\text{MnO}_3$  ( $x = 0.2, 0.3, 0.4$ ) at room temperature  $\times =$  (a) 0, (b) 0.1, (c) 0.2.

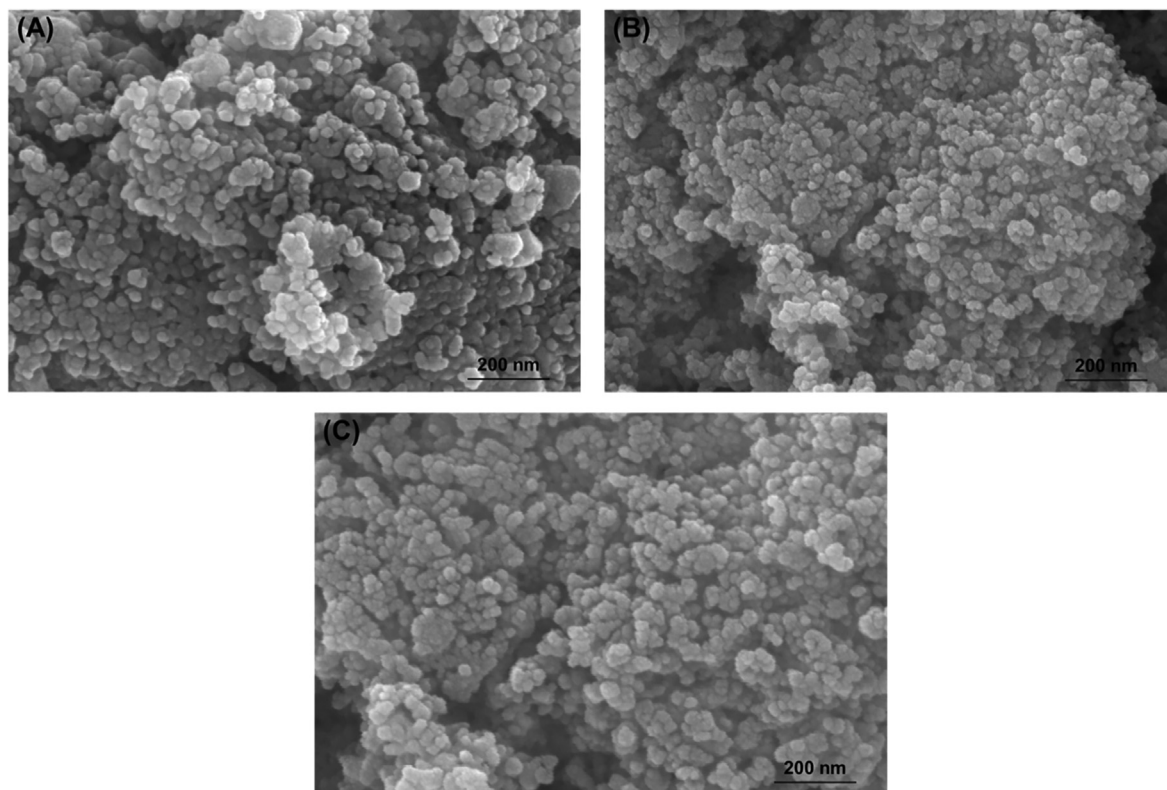


Fig. 2. SEM images of (A)  $\text{La}_{0.6}\text{Ba}_{0.4}\text{MnO}_3$ , (B)  $\text{La}_{0.7}\text{Ba}_{0.3}\text{MnO}_3$ , and (C)  $\text{La}_{0.8}\text{Ba}_{0.2}\text{MnO}_3$ .

Table 2  
BET analyses of the nanoparticles.

Parameter	Unit	$\text{La}_{0.6}\text{Ba}_{0.4}\text{MnO}_3$	$\text{La}_{0.7}\text{Ba}_{0.3}\text{MnO}_3$	$\text{La}_{0.8}\text{Ba}_{0.2}\text{MnO}_3$
BET surface area	( $\text{m}^2/\text{g}$ )	17.8617	20.4567	24.7480
Total volume in pores	( $\text{cm}^3/\text{g}$ )	0.03042	0.03547	0.04021
Total area in pores	( $\text{m}^2/\text{g}$ )	19.349	22.895	26.243

$$\text{Cell viability inhibition (\%)} = \left[ \frac{(A_{\text{control}} - A_{\text{sample}})}{A_{\text{control}}} \right] \times 100 \quad (3)$$

## 2.8. Biofilm inhibition activity

*S. aureus* and *P. aeruginosa* were used to examine the biofilm inhibition effect of newly synthesized lanthanum nanoparticles. Different concentrations of newly synthesized lanthanum nanoparticles were separately added into a 24-well plate contain NB medium. Then *S. aureus* and *P. aeruginosa* inoculation ( $3.2 \times 10^8$  CFU/mL) was done at 1% volume and then incubated at 37 °C for 72 h. When the incubation period was over, the wells were gently drained and washed twice with distilled water. Next, the plates were dried for 45 min at 60 °C, and biofilms were stained with crystal violet solution (1%) for 60 min. The crystal violet was then removed and the plates were washed gently with water. The washing step was done twice. The absorbed crystal violet was dissolved in ethanol (96%) and the absorbance determined by measuring at 595 nm with a spectrophotometer [19]. All experiments were tested at least triple. Wells containing only microorganisms and media were used as positive controls. Biofilm inhibition was calculated according to Eq. (4).

$$\text{Biofilm Inhibition (\%)} = \left( \frac{\text{Abs}(\text{control}) - \text{Abs}(\text{sample})}{\text{Abs}(\text{control})} \right) \times 100 \quad (4)$$

## 3. Results and discussion

### 3.1. Characterization of perovskite type $\text{La}_{1-x}\text{Ba}_x\text{MnO}_3$ nanoparticles

Fig. 1a–c show the refined XRD patterns of the  $\text{La}_{1-x}\text{Ba}_x\text{MnO}_3$  ( $x = 0.2, 0.3, 0.4$ ) compounds at room temperature. Red dots, black and thin black lines indicate the observed, calculated and difference of these patterns, respectively. In addition, the Bragg positions were shown below for each figure. The optimized structural parameters for the main phase and secondary phases, and  $S$  ( $\chi^2$  goodness of fit) are listed in Table 1. There is a good agreement between observed and calculated patterns according to  $\chi^2$  values. All samples crystallize in the rhombohedral structure (space group:  $R\text{-}3cH$ ). For  $x = 0.2$  and  $0.3$ , the samples have a main phase in the crystal structure but the secondary phase begins to grow up when the Ba amount increases from  $0.3$  to  $0.4$ . The results show that the dissolve of Ba in the perovskite decreases and the orthorhombic  $\text{Ba}_6\text{Mn}_5\text{O}_{16}$  structure (space group:  $Cmca$ ) begin to

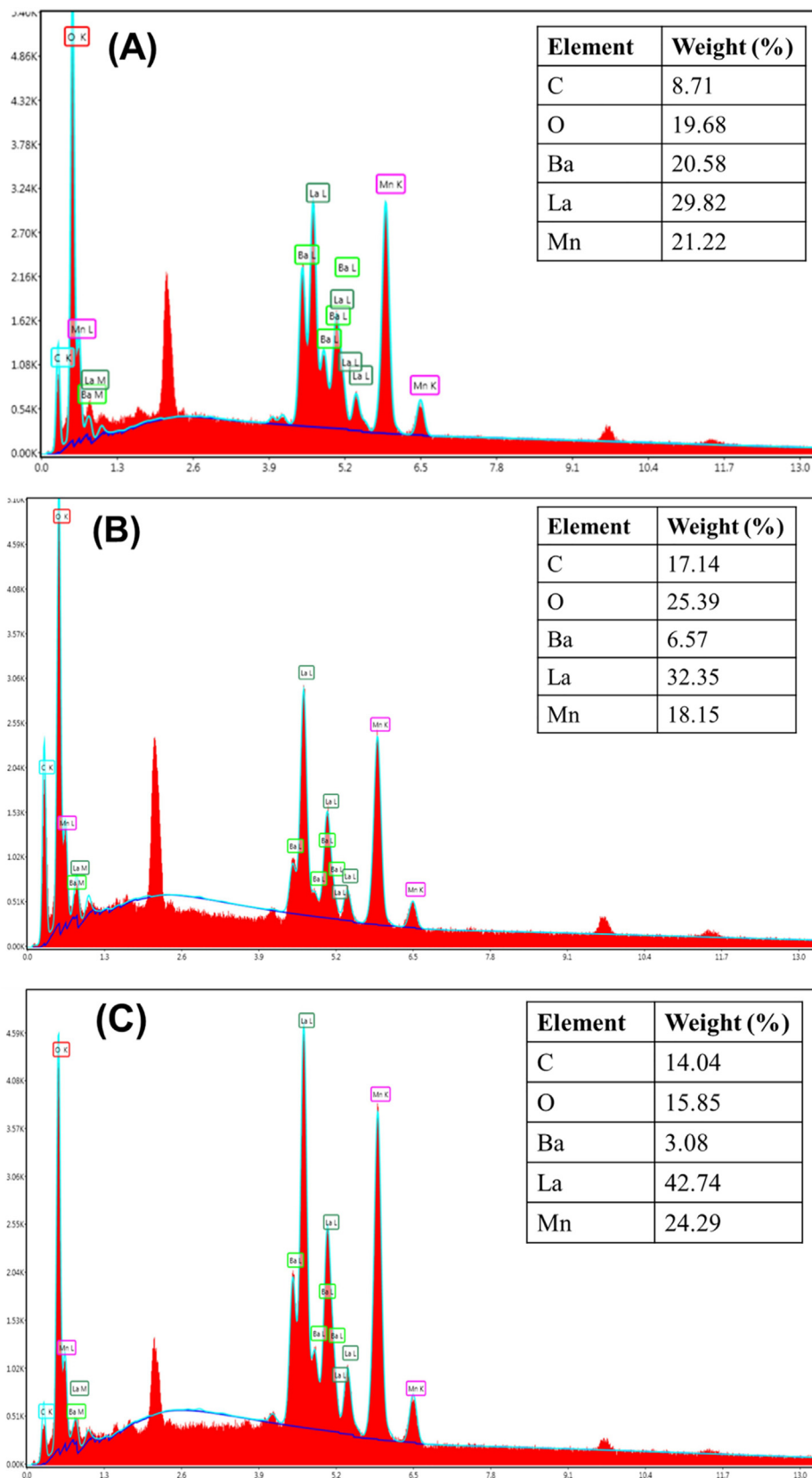


Fig. 3. EDX images of (A)  $\text{La}_{0.6}\text{Ba}_{0.4}\text{MnO}_3$ , (B)  $\text{La}_{0.7}\text{Ba}_{0.3}\text{MnO}_3$ , and (C)  $\text{La}_{0.8}\text{Ba}_{0.2}\text{MnO}_3$ .

occur in the pattern. The percentage of this phase is about 6.4 %. The lattice parameter slightly decreases when the Ba changes from 0.2 to 0.3 and, in the compound with 0.4 Ba, the orthorhombic

structure crystallizes inside the main phase. The results of this crystallization causes to increase the volume of the unit cell from 358.335 to 360.999 Å<sup>3</sup>.



The morphology of the  $\text{La}_{1-x}\text{Ba}_x\text{MnO}_3$  ( $x = 0.2, 0.3, 0.4$ ) compounds was characterized by SEM. In the Fig. 2, SEM image of  $\text{La}_{0.6}\text{Ba}_{0.4}\text{MnO}_3$ ,  $\text{La}_{0.7}\text{Ba}_{0.3}\text{MnO}_3$ , and  $\text{La}_{0.8}\text{Ba}_{0.2}\text{MnO}_3$  is shown. The image shows that nanocrystals are agglomerated, and the particles are spherical. The mean of the particles size from SEM image has been found about 30–50 nm.

The EDX of  $\text{La}_{0.6}\text{Ba}_{0.4}\text{MnO}_3$  compound showed the elementary components were composed of C (8.71 wt%), O (19.68 wt%), Ba (20.58 wt%), La (29.82 wt%), and Mn (21.22 wt%). EDX elemental spectra of the compounds confirmed the successful production of perovskite type  $\text{La}_{1-x}\text{Ba}_x\text{MnO}_3$  due to the presence of La, Ba and Mn. The results indicated that weight of La increased from 29.82 to 42.74 wt% when stoichiometric ratio of La increased from 0.6 to 0.8 in the compound. However, weight of Ba decreased from 20.58 to 3.08 wt% when stoichiometric ratio of Ba decreased from 0.4 to 0.2 in the compound.

The surface areas for the different compounds of perovskite type of  $\text{La}_{1-x}\text{Ba}_x\text{MnO}_3$  nanoparticles were measured using the adsorption and desorption experiments of nitrogen gas. In addition, the total pore volume, the micro pore volume and the pore diameter were measured. BET analysis for  $\text{La}_{0.6}\text{Ba}_{0.4}\text{MnO}_3$ ,  $\text{La}_{0.7}\text{Ba}_{0.3}\text{MnO}_3$ , and  $\text{La}_{0.8}\text{Ba}_{0.2}\text{MnO}_3$  compounds are summarized in Table 2.

The surface area of the nanoparticles increased with the increase of La ratio in the compounds. The surface area increased from 17.8617  $\text{m}^2/\text{g}$  for  $\text{La}_{0.6}\text{Ba}_{0.4}\text{MnO}_3$  to 24.7480  $\text{m}^2/\text{g}$  for  $\text{La}_{0.8}\text{Ba}_{0.2}\text{MnO}_3$ . The total volume and the total area in pores are also directly proportional to the La ratio in the compounds.

### 3.2. DPPH radical scavenging activity

Reactive oxygen species (ROS) is a type of oxygen that reacts and damages cells. It can be controlled by an oxidative inhibition agent called an antioxidant [20]. Therefore, an antioxidant property of a newly synthesized substance is an important feature of that compound. DPPH free radical activity of perovskite nanoparticles was carried out at various concentrations (range from 25 to 500 mg/L). Ascorbic acid and Trolox used as standard. Ascorbic acid and Trolox showed the highest DPPH radical scavenging activity at all concentrations. The DPPH free radical inhibition rate of the nanoparticles increases by increasing the concentration as shown in Fig. 3. The order of the free radical scavenging activity was  $\text{La}_{0.6}\text{Ba}_{0.4}\text{MnO}_3 > \text{La}_{0.7}\text{Ba}_{0.3}\text{MnO}_3 > \text{La}_{0.8}\text{Ba}_{0.2}\text{MnO}_3$  at concentration of 500 mg/L. When the concentration increased from 250 mg/L to 500 mg/L, the scavenging activities of  $\text{La}_{0.6}\text{Ba}_{0.4}\text{MnO}_3$ ,  $\text{La}_{0.7}\text{Ba}_{0.3}\text{MnO}_3$ , and  $\text{La}_{0.8}\text{Ba}_{0.2}\text{MnO}_3$  were increased from 35.59% to 46.54%, from 29.55% to 39.62% and from 20.25% to 34.84%, respectively. Chakraborty et al [21] reported that they synthesized lanthanum nanoparticle and it was showed DPPH scavenging activity. Kumar et al. [22] studied the antioxidant activity of lanthanum nanoparticles with DPPH test. They reported that lanthanum nanoparticles showed good DPPH free radical scavenging activity. Our results demonstrated parallel with this investigation. In our study, the nanoparticle  $\text{La}_{0.6}\text{Ba}_{0.4}\text{MnO}_3$  showed the highest inhibitory activity with 46.54% (see Fig. 4).

### 3.3. Ferrous ion chelating activity

The antioxidant activities of the nanoparticles were also measured using the  $\text{Fe}^{2+}$  chelating methods. The result of chelating activity of the nanoparticles is depicted in Fig. 5. As seen in Fig. 5, it was observed that the chelating activity increased depending on the concentration. According to the results,  $\text{Fe}^{2+}$  chelating activity rate of  $\text{La}_{0.6}\text{Ba}_{0.4}\text{MnO}_3$ ,  $\text{La}_{0.7}\text{Ba}_{0.3}\text{MnO}_3$ , and  $\text{La}_{0.8}\text{Ba}_{0.2}\text{MnO}_3$  at concentrations of 25–500 mg/L ranged from 16% to 67%, from 13% to 66% and from 9% to 46%, respectively.  $\text{La}_{0.6}\text{Ba}_{0.4}\text{MnO}_3$  exhib-

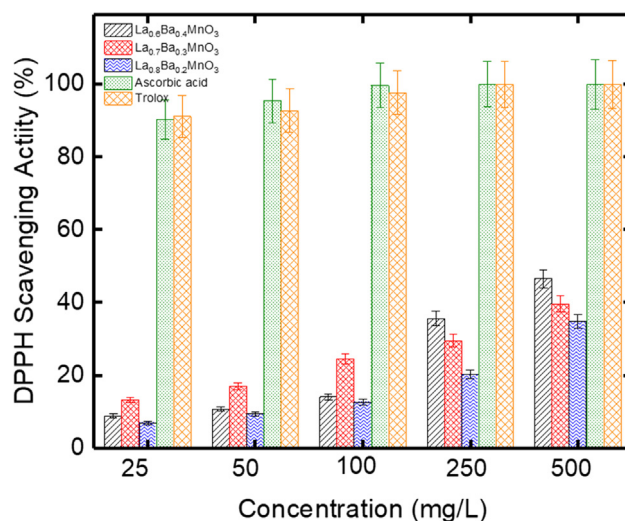


Fig. 4. DPPH scavenging activity.

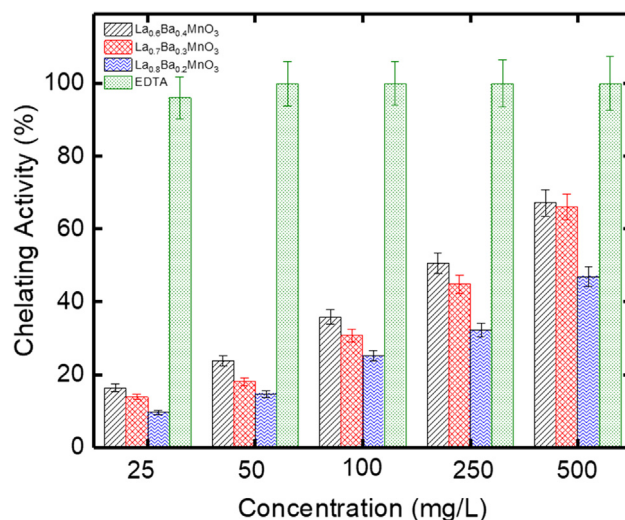


Fig. 5. Ferrous ion chelating activity.

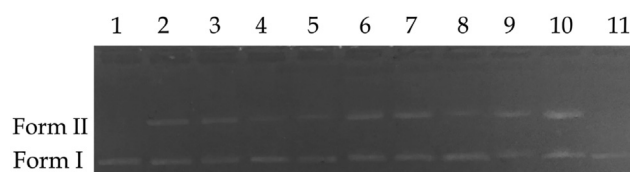


Fig. 6. DNA cleavage of lanthanum nanoparticles (Lane 1, pBR 322 DNA; Lane 2, pBR 322 DNA + 125 mg/L of 6; Lane 3, pBR 322 DNA + 250 mg/L of 6; Lane 4, pBR 322 DNA + 500 mg/L of 6; Lane 5, pBR 322 DNA + 125 mg/L of 7; Lane 6, pBR 322 DNA + 250 mg/L of 7; Lane 7, pBR 322 DNA + 500 mg/L of 7; Lane 8, pBR 322 DNA + 125 mg/L of 8; Lane 9, pBR 322 DNA + 250 mg/L of 8; Lane 10, pBR 322 DNA + 500 mg/L of 8; Lane 11, pBR 322 DNA + DMSO).

ited the highest activity at all concentrations among the tested nanoparticles and chelating activities of  $\text{La}_{0.6}\text{Ba}_{0.4}\text{MnO}_3$  at concentrations of 25 mg/L, 50 mg/L, 100 mg/L, 250 mg/L and 500 mg/L were 16.38%, 23.72%, 35.87%, 50.56%, and 67.23%, respectively. The order of the ferrous iron chelating activities was  $\text{EDTA} > \text{La}_{0.6}\text{Ba}_{0.4}\text{MnO}_3 > \text{La}_{0.7}\text{Ba}_{0.3}\text{MnO}_3 > \text{La}_{0.8}\text{Ba}_{0.2}\text{MnO}_3$  and they were also showed 100%, 67.23%, 66.10%, and 46.89% ferrous ion chelating activities, respectively at 500 mg/L. These results demonstrated

that the nanoparticles especially  $\text{La}_{0.6}\text{Ba}_{0.4}\text{MnO}_3$  can be used as chelating agent.

### 3.4. DNA cleavage ability

The cleavage activity perovskite nanoparticles to the plasmid pBR322 DNA was monitored by gel electrophoresis. Fig. 6 shows gel electrophoretic division of pBR322 DNA after incubation with different concentrations of the nanoparticles. The cleavage efficiency of nanoparticles was measured by determining the ability of the compounds to convert the supercoiled (SC) DNA to the nicked circular (NC) form (cleavage). When pBR322 plasmid DNA was interacted with the nanoparticles Form I was broken and the intensity of Form II DNA increased. The results showed that lanthanum nanoparticles caused breakings on DNA strand behaving as a chemical nuclease. Asadi et al. [23] reported that they synthesized and characterized two water-soluble mono-nuclear lanthanum (III) complexes. They also studied DNA cleavage ability and these compounds showed nuclease activity. Our results are consistent with their findings. DNA is the target molecule for many drugs especially antitumor and anticancer drugs [23]. Therefore, the effect of nanoparticles on DNA suggests that newly synthesized  $\text{La}_{0.6}\text{Ba}_{0.4}\text{MnO}_3$ ,  $\text{La}_{0.7}\text{Ba}_{0.4}\text{MnO}_3$ , and  $\text{La}_{0.8}\text{Ba}_{0.2}\text{MnO}_3$  can be used as chemical nuclease agents after following studies.

### 3.5. Antimicrobial activity

*In vitro* antimicrobial potentials of the nanoparticles were studied in terms of minimum inhibition concentration (MIC) value against various pathogen microorganisms (Table S1). According

to our results, the nanoparticles were more effective on Gr (+) bacteria and yeasts than Gr (-) bacteria. *C. tropicalis* was the most affected species by the nanoparticles and MIC values were 4  $\mu\text{g/mL}$ , 8  $\mu\text{g/mL}$  and 16  $\mu\text{g/mL}$  for  $\text{La}_{0.7}\text{Ba}_{0.4}\text{MnO}_3$ ,  $\text{La}_{0.6}\text{Ba}_{0.4}\text{MnO}_3$ , and  $\text{La}_{0.8}\text{Ba}_{0.2}\text{MnO}_3$  nanoparticles, respectively.  $\text{La}_{0.7}\text{Ba}_{0.4}\text{MnO}_3$  was determined as the most effective nanoparticle against test microorganisms except *E. coli* and MIC values were 64  $\mu\text{g/mL}$ , 16  $\mu\text{g/mL}$ , 64  $\mu\text{g/mL}$ , 32  $\mu\text{g/mL}$ , 64  $\mu\text{g/mL}$ , 4  $\mu\text{g/mL}$ , and 32  $\mu\text{g/mL}$  for *P. aeruginosa*, *L. pneumophila*, *E. hirae*, *E. fecalis*, *S. aureus*, *C. parapsilosis*, and *C. tropicalis*, respectively. The effects of nanoparticles on microorganisms can be by different mechanisms for example, in the antibacterial activity of AgNPs, events such as enzyme degradation, cell protein inactivation and DNA breakdown may have an effect on cell death [24]. Jadhav and Khetre [25] indicated that they studied the effect of  $\text{LaNiO}_3$  nanoparticle and it showed antibacterial activity against *Staphylococcus aureus* but  $\text{LaNiO}_3$  did not exhibit antibacterial activity for *Streptococcus* spp., *B. subtilis*, *E. coli*, and antifungal activity for *C. albicans*. Manjunatha et al. [26] reported that perovskite lanthanum aluminate nanoparticles showed antimicrobial activity and MIC value was 63  $\mu\text{g/mL}$ , and 70  $\mu\text{g/mL}$  against *P. aeruginosa* and *E. coli*, respectively. The results obtained were almost the same as their findings. As a result, they can be used as an antibacterial agent after further studies.

### 3.6. Biofilm inhibition activity

Bacteria in biofilms have a number of properties that make them difficult to eradicate. They are phenotypically different from

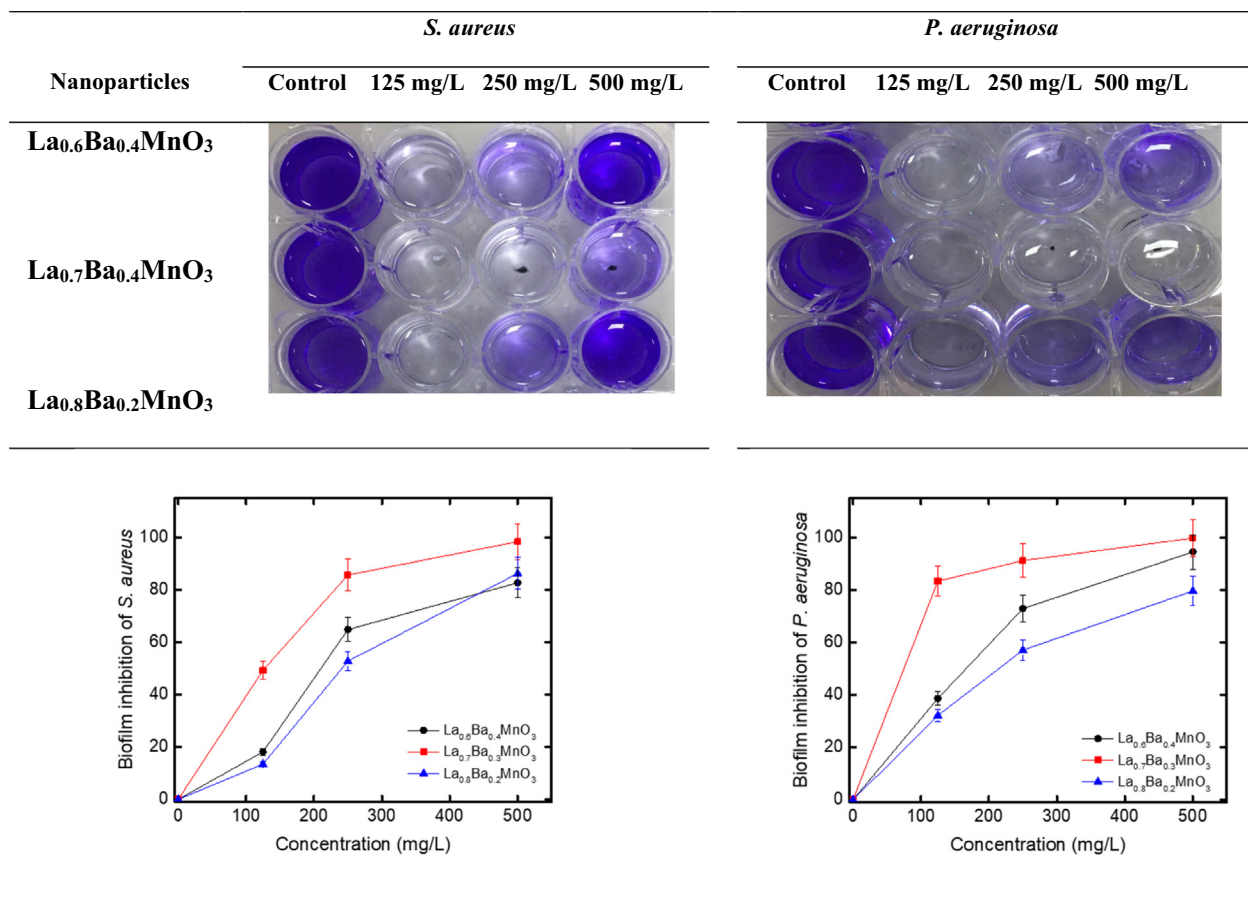
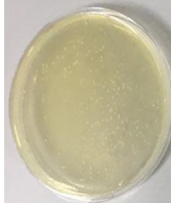
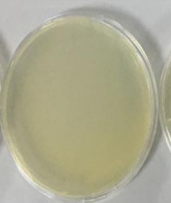
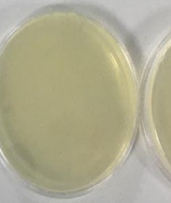
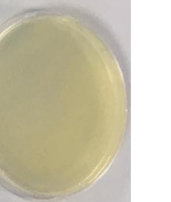
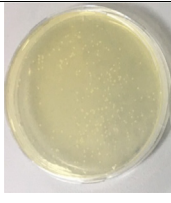
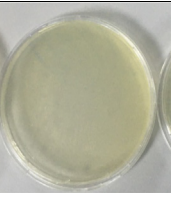
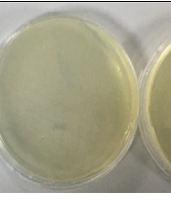
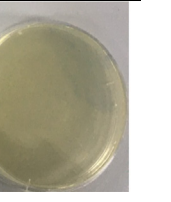


Fig. 7. Biofilm inhibition of perovskite lanthanum nanoparticles.

**Table 3**  
Cell viability.

Time	Control	La <sub>0.6</sub> Ba <sub>0.4</sub> MnO <sub>3</sub>	La <sub>0.7</sub> Ba <sub>0.4</sub> MnO <sub>3</sub>	La <sub>0.8</sub> Ba <sub>0.2</sub> MnO <sub>3</sub>
After 30 min				
After 60 min				

their planktonic counterparts, especially with regard to gene expression and growth rates. Biofilms are inherently resistant to antibiotics and are upwards of 1000-fold more resistant to them than planktonic bacteria [27]. Also, bacterial biofilms are connected with a broad range of infections and chronic tissue infections. It causes shortening of the life of exogenous devices such as prosthetic joints or catheters.[28]. For these reasons, various strategies are required to prevent the formation of biofilm. In this investigation, biofilm inhibition percentages of lanthanum nanoparticles were examined against *S. aureus* and *P. aeruginosa* (Fig. 7). Inhibition rates of La<sub>0.6</sub>Ba<sub>0.4</sub>MnO<sub>3</sub>, La<sub>0.7</sub>Ba<sub>0.4</sub>MnO<sub>3</sub>, and La<sub>0.8</sub>Ba<sub>0.2</sub>MnO<sub>3</sub> at 250 mg/L concentration were determined as 64.85%, 85.65%, and 52.75% against *S. aureus* respectively and 72.93%, 91.19%, and 57.08%, against *P. aeruginosa* respectively. The biofilm inhibition percentages of nanoparticles against *P. aeruginosa* and *S. aureus* were La<sub>0.7</sub>Ba<sub>0.4</sub>MnO<sub>3</sub> > La<sub>0.6</sub>Ba<sub>0.4</sub>MnO<sub>3</sub> > La<sub>0.8</sub>Ba<sub>0.2</sub>MnO<sub>3</sub> at all concentrations. When the concentration of La<sub>0.7</sub>Ba<sub>0.4</sub>MnO<sub>3</sub> increased from 125 mg/L to 500 mg/L, the inhibition percentages were found to increase from 49.28% to 98.38% and 83.38% to 99.78%, against *S. aureus* and *P. aeruginosa*, respectively. According to these results, newly synthesized lanthanum nanoparticles were quite effective on both microorganisms. The results suggested that lanthanum nanoparticles had strong biofilm inhibition activity against *S. aureus* and *P. aeruginosa*, so they can be used as antibiofilm agents.

### 3.7. Bacterial viability effect

Since the dawn of human history, people have suffered from infectious diseases. *E. coli* is a common pathogen that causes various infectious diseases. The multidrug-resistance of bacteria against antibiotics also makes treatment difficult with each passing day. Therefore, it is urgent to develop new treatment strategies for effective antibacterial treatment [16]. The results of cell viability of *E. coli* compared to the control group are shown in Table 2. According to our results, it was observed that each lanthanum nanoparticles killed 100% of *E. coli* bacteria at the end of 30 and 60 min. Gao et al. [16] found that La(III) complex may act on the cell envelope of bacteria to achieve good bactericidal effects. The 100% bactericidal effect of the newly synthesized lanthanum

nanoparticles can be explained by this situation. In addition, our results showed that our newly synthesized lanthanum nanoparticles may contribute to the development of antimicrobial drugs after various toxicology test processes (see Table 3).

## 4. Conclusion

In this study, we synthesized perovskite type La based La<sub>1-x</sub>Ba<sub>x</sub>MnO<sub>3</sub> (x = 0.2, 0.3, 0.4) nanoparticle by Sol-gel technic. According to our results, perovskite nanoparticles showed good antioxidant activity. DNA cleavage activity results showed that pBR322 plasmid DNA (Form I) was broken and the intensity of Form II DNA increased and the nanoparticles cause breakings on DNA strand behaving as a chemical nuclease. The nanoparticles showed effective antimicrobial activity and La<sub>0.7</sub>Ba<sub>0.4</sub>MnO<sub>3</sub> also was the most effective one. The nanoparticles exhibited strong biofilm inhibition activity against *S. aureus* and *P. aeruginosa* nearly 100%. After the cell viability test against *E. coli*, they demonstrated 100% antibacterial ability. The present study provides useful information on the biological activities of the nanoparticles, which may be useful for the rational design of novel nanodrugs.

## Declaration of Competing Interest

The authors declare that they have no known competing financial interests or personal relationships that could have appeared to influence the work reported in this paper.

## Appendix A. Supplementary data

Supplementary data to this article can be found online at <https://doi.org/10.1016/j.appt.2021.10.038>.

## References

- [1] Z.M. Wang, J.J. Jiang, Magnetic entropy change in perovskite manganite La<sub>(0.7)A<sub>(0.3)</sub>MnO<sub>(3)</sub></sub> La<sub>(0.7)A<sub>(0.3)</sub>Mn<sub>(0.9)Cr<sub>(0.1)</sub>O<sub>(3)</sub></sub> (A = Sr, Ba, Pb) and Banerjee criteria on phase transition, Solid State Sci. 18 (2013) 36–41.</sub>
- [2] V.K. Pecharsky, K.A. Gschneidner, Effect of alloying on the giant magnetocaloric effect of Gd-5(Si<sub>2</sub>Ge<sub>2</sub>), J. Magn. Magn. Mater. 167 (3) (1997) L179–L184.



- [3] M.-H. Phan, S.-C. Yu, Review of the magnetocaloric effect in manganite materials, *J. Magn. Magn. Mater.* 308 (2) (2007) 325–340.
- [4] I. Kucuk, A. Tekgül, K. Sarlar, E. Civan, N. Kucuk, B. Macan, Synthesis and characterization of graphene nanoplatelet-La<sub>0.7</sub>Ca<sub>0.3</sub>MnO<sub>3</sub> composites, *Phil. Mag.* 99 (21) (2019) 2736–2750.
- [5] L. Malvasia, C. Ritter, M.C. Mozzati, C. Tealdi, M.S. Islamd, C.B. Azzoni, G. Flor, *J. Solid State Chem.* 178 (2005) 2042.
- [6] L. Malvasia, *J. Mater. Chem.* 18 (2008) 3295.
- [7] S. Hébert, B. Wang, A. Maignan, C. Martin, R. Retoux, B. Raveau, *Solid State Commun.* 123 (2002) 311.
- [8] A. Arroyo, J.M. Alonso, R. Cortés-Gil, J.M. Gonzalez-Calbet, A. Hernando, J.M. Rojo, M. Vallet-Regí, *Magn. J. Magn. Mater.* 272 (2004) 1748.
- [9] C. Singh, A. Wagle, M. Rakesh, Doped LaCoO<sub>3</sub> perovskite with Fe: A catalyst with potential antibacterial activity, *Vacuum* 146 (2017) 468–473.
- [10] W. Wang, M.O. Tadó, Z. Shao, Research progress of perovskite materials in photocatalysis-and photovoltaics-related energy conversion and environmental treatment, *Chem. Soc. Rev.* 44 (15) (2015) 5371–5408.
- [11] Ünlü, C.G. Tanış, E. Y. Kaynar, B., Şimşek, T., Özcan, Ş., Magnetocaloric effect in La<sub>0.7</sub>NdxBa(0.3-x)MnO<sub>3</sub> (x= 0, 0.05, 0.1) perovskite manganites, *Journal of Alloys and Compounds*, 704 (2017) 58-63.
- [12] A. Tekgül, C.G. Ünlü, K. Sarlar, İ. Küçük, The structural, magnetic and magnetocaloric properties of La<sub>0.7</sub>KxCa<sub>0.3-x</sub>MnO<sub>3</sub> (x=0, 0.05, 0.1) perovskite compounds, *J. Mater. Sci. Mater. Electron.* 31 (2020) 6875–6882.
- [13] S. Behera, S. Jha, M. Arakha, T. Panigrahi, Synthesis of Silver Nanoparticles from microbial source-a green synthesis approach and evaluation of its antimicrobial activity against *Escherichia coli*, *Int. J. Eng. Res. Appl.* 3 (2013) 58–62.
- [14] M. Mahdavi et al., Synthesis, surface modification and characterisation of biocompatible magnetic iron oxide nanoparticles for biomedical applications, *Molecules* 18 (2013) 7533–7548.
- [15] M. Arakha, S. Pal, D. Samantarrai, et al., Antimicrobial activity of iron oxide nanoparticle upon modulation of nanoparticle-bacteria interface, *Sci. Rep.* 5 (2015) 14813.
- [16] S. Gao, M. Huang, Z. Sun, D. Li, C. Xie, L. Feng, S. Liu, K. Zheng, Q. Pang, A new mixed-ligand lanthanum (III) complex with salicylic acid and 1,10-phenanthroline: Synthesis, characterization, antibacterial activity, and underlying mechanism, *J. Mol. Struct.* 1225 (2021) 129096, <https://doi.org/10.1016/j.molstruc.2020.129096>.
- [17] M. Salih Ağırtaş, C. Karataş, S. Özdemir, Synthesis of some metallophthalocyanines with dimethyl 5- (phenoxy) -isophthalate substituents and evaluation of their antioxidant-antibacterial activities, *Spectrochim. Acta Part A Mol. Biomol. Spectrosc.* 135 (2015) 20–24.
- [18] T.C.P. Dinis, V.M.C. Madeira, L.M. Almeida, Action of phenolic derivatives (acetaminophen, salicylate, and 5-aminosalicylate) as inhibitors of membrane lipid peroxidation and as peroxy radical scavengers, *Arch. Biochem. Biophys.* 315 (1) (1994) 161–169.
- [19] S. Stepanović, D. Vuković, I. Dakić, B. Savić, M. Švabić-Vlahović, A modified microtiter-plate test for quantification of staphylococcal biofilm formation, *J. Microbiol. Methods* 40 (2) (2000) 175–179.
- [20] G. Maheshwaran, R. Selva Muneeswari, A. Nivedhitha Bharathi, M. Krishna Kumar, S. Sudhahar, Eco-friendly synthesis of lanthanum oxide nanoparticles by *Eucalyptus globulus* leaf extracts for effective biomedical applications, *Mater Lett.* 283 (1) (2021) 1–4.
- [21] P. Chakraborty, D. Dam, J. Abraham, Bioactivity of Lanthanum Nanoparticle Synthesized using *Trigonella foenum-graecum* Seed Extract, *J. Pharm. Sci. & Res.* 8 (11) (2016) 1253–1257.
- [22] K.A. Manoj Kumar, E. Hemanathan, P. Renuka Devi, S. Vignesh Kumar, R. Hariharan, Biogenic synthesis, characterization and biological activity of lanthanum nanoparticles, *Mater. Today Proc.* 21 (2020) 887–895.
- [23] Z. Asadi, N. Nasrollahi, H. Karbalaie-Heidari, V. Eigner, M. Dusek, N. Mobaraki, R. Pournejati, Investigation of the complex structure, comparative DNA-binding and DNA cleavage of two water-soluble mono-nuclear lanthanum(III) complexes and cytotoxic activity of chitosan-coated magnetic nanoparticles as drug delivery for the complexes, *Spectrochim Acta - Part A Mol. Biomol. Spectrosc.* 178 (2017) 125–135.
- [24] S. Husain, S.K. Verma, Hemlata, M. Azam, M. Sardar, Q.M.R. Haq, T. Fatma, Antibacterial efficacy of facile cyanobacterial silver nanoparticles inferred by antioxidant mechanism, *Mater. Sci. Eng. C* 122 (2021) 111888, <https://doi.org/10.1016/j.msec.2021.111888>.
- [25] A.L. Jadhav, S.M. Khetre, Antibacterial activity of LaNiO<sub>3</sub> prepared by sonicated sol gel method using combination fuel, *International, Nano Lett.* 10 (1) (2020) 23–31.
- [26] C.R. Manjunatha, B.M. Nagabhushana, M.S. Raghu, S. Pratibha, N. Dhananjaya, A. Narayana, Perovskite lanthanum aluminate nanoparticles applications in antimicrobial activity, adsorptive removal of Direct Blue 53 dye and fluoride, *Mater. Sci. Eng. C* 101 (2019) 674–685.
- [27] J.L. Del Pozo, Biofilm-related disease, *Expert Rev. Anti. Infect. Ther.* 16 (1) (2018) 51–65.
- [28] O. Ciofu, E. Rojo-Moliner, M.D. Macià, A. Oliver, Antibiotic treatment of biofilm infections, *Apmis* 125 (4) (2017) 304–319.